PHYSICAL REVIEW B VOLUME 18, NUMBER 8 15 OCTOBER 1978

Effect of an impurity on interband optical absorption in solids*

J. C. Parlebas† and D. L. Mills
Department of Physics, University of California, Irvine, California 92717
(Received 4 April 1977)

We explore the effect of an impurity on the contribution to the optical absorption in solids from electronic interband transitions. We view the impurity as a point probe which, through breakdown of wave-vector conservation, allows the incoming photon to probe critical points in the pure-crystal band structure not accessible by optical methods in the pure solid. After formulating the problem in a general manner, we present numerical studies of a one-dimensional two-band solid to illustrate how the impurity can "activate" critical points in the host band structure.

I. INTRODUCTION

The study of the optical-absorption spectrum of solids is a primary means of obtaining information about the electronic band structure of materials. While there has been a very considerable theoretical effort directed toward the calculation of optical-absorption spectra for a wide variety of pure materials, rather little attention has been devoted to this question for impure solids or alloys.

The purpose of the present paper is to examine the effect of a single impurity on the electronic interband absorption spectrum of a solid. One role an impurity may play is to "activate" indirect transitions between critical points of the host band structure through breakdown of wave-vector conservation. Thus, the study of optical absorption in solids doped with a small concentration of impurities may provide information about host band structures richer in content than the absorption spectrum of the pure material. It is this aspect of impurity-induced optical absorption we wish to study here. We remark that in the infrared region of the spectrum, the use of impurities to activate critical points in the host-phonon density of states has been utilized both in absorption and Raman studies of lightly doped solids.[1] With the exception of the paper by Velicky and Levin,[2] discussed in more detail below, this aspect of impurity-induced electronic absorption has not been examined by theorists, as far as we know. We believe this area is potentially very useful, and deserves further theoretical study.

As remarked above, theoretical studies of optical absorption by electrons in impure solids seem few in number. Some years ago, Caroli[3] presented an analysis of optical absorption by electrons in a dilute alloy that can be described by the Friedel-Anderson model. That is, the host has a nearly-free-electron conduction band, and a localized orbital is associated with the impurity site. This localized state broadens into a virtual level through admixing with the conduction band. The absorption processes studied by Caroli are necessarily wave-vector nonconserving. However, since Caroli presumed the host conduction band to have a structureless density of states, Caroli's study shows how optical absorption may be used to probe the nature of the virtual level on the impurity site. The emphasis is thus very different than that described in our earlier remarks. We remark that Caroli's results have proved most useful in the analysis of optical data on dilute alloys with well-defined virtual levels.[4] Kjöllerström[5] has also investigated a model very similar in physical content to Caroli's, through use of rather formal theoretical techniques. More recently, Bennett and Penn[6] have examined a more general model which includes interband transitions. Their model also makes essential use of a localized orbital at the impurity site, and they present no detailed discussion of the processes of interest to us.

These models which focus on absorption mediated by an isolated orbital on the impurity are useful for a wide class of alloys. An example is dilute *Cu*Ni, where the Ni impurity has a sharp virtual level between the top of the *d* band and the Fermi level.[4] However, for photon energies large enough to lift an electron from the copper *d* bands to above the Fermi level, no sharp virtual level is seen by photons which excite electrons from the copper *d* bands. Wave-vector nonconserving transitions originate from this energy region nonetheless. It is these processes that should in principle serve as a probe of the host band structure. We use the *Cu*Ni system as an example here; for a wide variety of metallic systems we may expect sharp virtual levels to be absent, yet optical studies of alloys may yield important information about the electronic structure of the material.

A paper by Velicky and Levin[2] addresses questions very similar to those that motivated the present study. These authors examine the frequency

variation of the conductivity of a model alloy with a single, tight-binding conduction band in the host. This conduction band has Van Hove critical points, and their calculations show weak but nonetheless clear structure produced by impurity-induced indirect transitions from critical points in the host band structure to the vicinity of the Fermi level. We find it most encouraging to see this structure present for calculations carried out for a model with Van Hove singularities of a gentle sort. From an experimental point of view, derivative spectroscopy can be used to enhance such features in data.

Our study, reported here, is rather different than that of Velicky and Levin. They calculate the frequency-dependent conductivity of an alloy with a finite concentration of impurities by first obtaining the "average medium" one-electron Green's function with the coherent potential approximation (CPA). The conductivity is related to a two-particle Green's function by a well-known Kubo formula, and Velicky and Levin use an approximate decoupling scheme which replaces the average two-particle Green's function by a convolution over the single-particle average medium propagators. In the limit of low concentration, their procedure does not produce the exact result for the one-impurity problem that forms the basis for the present treatment. We prefer to begin our analysis of this phenomenon by treating the one-impurity problem fully, to obtain features in the absorption spectrum that are correct in the limit of low concentration, and we do not address the question of extending the theory to finite concentrations; the procedure used by Velicky and Levin is surely a reasonable, approximate approach.

Our interest in this problem has been stimulated by experimental studies of the *Ni*Cu system reported by Tokumoto *et al.*[7] Upon introducing a small concentration of Cu impurities into the Ni matrix, these authors find clear structure in a regime of photon energies where the initial states in the absorption process are inside the host Ni *d* bands. This structure may provide a measure of the Stoner splitting of the *d* bands in the ferromagnetic Ni matrix, although data on the temperature dependence of the observed structure would be helpful in deciding whether this is so. It is intriguing to suppose that through study of the optical spectra of dilute alloys, one may probe properties of the host band structure inaccessible by optical studies of the host itself, and it is this consideration that prompts us to examine the question.

The outline of this paper is as follows. In Sec. II, we derive a rather general expression for $\epsilon_2(\omega)$, the imaginary part of the dielectric constant of an impure solid. Then we apply the general expression to a model of a two-band solid, and explore some of its features. The two-band model is a model of an insulating material, but very similar considerations apply to metals also. In Sec. III, we discuss a series of numerical studies of the model. These studies show that the impurity-induced indirect transitions indeed produce structure in the optical spectrum that reflect critical points in the host band structure. In Sec. IV, we give a brief discussion of our results. At the moment, we are extending the analysis to more realistic three-dimensional crystal models.

II. GENERAL REMARKS

We begin by writing the general expression for $\epsilon_2(\omega)$, the imaginary part of the dielectric constant, for a material with cubic symmetry illuminated with radiation of frequency ω. Then by proceeding quite generally, we cast the expression in a form suitable for one-electron theory. The section concludes with further remarks on the relation between our approach and that of Ref. 2, and casts the expresion for $\epsilon_2(\omega)$ into the form that will form the basis for the numerical studies of Sec. III.

Our discussion will be entirely within the framework of one-electron theory. Then (in units with $\hbar = 1$) quite generally $\epsilon_2(\omega)$ is given by the expression

$$\epsilon_2(\omega) = \frac{4\pi^2 e^2}{Vm^2} \frac{1}{\omega^2} \sum_{ij} |\langle j|p_x|i\rangle|^2 (f_i - f_j) \times \delta(\epsilon_j - \epsilon_i - \omega) . \tag{2.1}$$

In this expression V is the volume of the crystal, m the free-electron mass, i and j are quantum numbers that label the one-electron eigenstates of energy ϵ_i and ϵ_j, p_x the x component of the momentum operator, and $f_i = (e^{\beta(\epsilon_i - \mu)} + 1)^{-1}$ is the Fermi-Dirac distribution function, with $\beta = (k_B T)^{-1}$.

If we define $S(z)$, a function of the complex variable z, by the statement

$$S(z) = \sum_{ij} \frac{|\langle j|p_x|i\rangle|^2}{\epsilon_j - \epsilon_i - z} (f_i - f_j) , \tag{2.2}$$

then

$$\epsilon_2(\omega) = \frac{4\pi e^2}{Vm^2} \frac{1}{\omega^2} \mathrm{Im}[S(\omega + i\eta)] , \tag{2.3}$$

where η is a positive infinitesimal.

If we have a dilute alloy, it is convenient to expand the exact one-electron eigenfunction of the alloy in terms of the Bloch functions of the host matrix. These Bloch functions form a complete set, and the Bloch function with wave vector $\vec{k}$ from band n will be denoted by $|n\vec{k}\rangle$. We then have

$$|i\rangle = \sum_n \sum_{\vec{k}} |n\vec{k}\rangle\langle n\vec{k}|i\rangle , \tag{2.4}$$

and a standard manipulation may be used to cast $S(z)$ into the form, with $i\omega_n = 2\pi k_B T(n+\frac{1}{2})$,

$$S(z) = \frac{1}{\beta} \sum_{i\omega_n} \sum_{n,\ldots,n'''} \sum_{\vec{k}\vec{k}'} \langle n''\vec{k}'|p_x|n'''\vec{k}'\rangle\langle n'\vec{k}|p_x|n\vec{k}\rangle G(n\vec{k},n''\vec{k}';i\omega_n) G(n'''\vec{k}',n'\vec{k};i\omega_n+z) . \tag{2.5}$$

In Eq. (2.5), if H is the Hamiltonian of the one-electron problem, we define the one-electron Green's function $G(n\vec{k},n'\vec{k}';z)$ through the relation

$$G(n\vec{k},n'\vec{k}';z) = \langle n\vec{k}|[1/(H-z)]|n'\vec{k}'\rangle . \tag{2.6}$$

To obtain Eq. (2.5), it is important to note that in the Bloch representation, the momentum matrix element is diagonal in the wave vector:

$$\langle n\vec{k}|p_x|n'\vec{k}'\rangle = \delta_{\vec{k}\vec{k}'}\langle n\vec{k}|p_x|n'\vec{k}\rangle . \tag{2.7}$$

This fact has a very important influence over the structure of Eq. (2.5), and makes the numerical evaluation of it quite tricky, as we will appreciate later.

The sum over $i\omega_n$ in Eq. (2.5) may be evaluated by standard contour integration methods. We shall need to know the Green's function $G(n\vec{k},n'\vec{k}';z)$ just above and just below the real axis after this is done. To express the result in convenient form, we write

$$G(n\vec{k},n'\vec{k}';\epsilon \pm i\eta) = G_p(n\vec{k},n'\vec{k}';\epsilon) \pm i\pi\rho(n\vec{k},n'\vec{k}';\epsilon) , \tag{2.8}$$

so that $\rho(n\vec{k},n'\vec{k}';\epsilon)$ gives the discontinuity of G across the real axis. It is quite important to note that in general $G_p(n\vec{k},n'\vec{k}';\epsilon)$ and $\rho(n\vec{k},n'\vec{k}';\epsilon)$ are not real. One may establish the identities

$$G_p(n\vec{k},n'\vec{k}';\epsilon) = G_p(n'\vec{k}',n\vec{k};\epsilon)^* , \tag{2.9a}$$

$$\rho(n\vec{k},n'\vec{k}';\epsilon) = \rho(n'\vec{k}',n\vec{k};\epsilon)^* , \tag{2.9b}$$

so only the diagonal parts $G_p(n\vec{k},n\vec{k};\epsilon)$ and $\rho(n\vec{k},n\vec{k};\epsilon)$ of these objects can be shown to be real.

After a standard contour integration, for $S(\omega+i\eta)$ we find

$$S(\omega+i\eta) = \sum_{n,\ldots,n'''} \sum_{\vec{k}\vec{k}'} \int_{-\infty}^{+\infty} d\epsilon\, f(\epsilon)\langle n''\vec{k}'|p_x|n'''\vec{k}'\rangle\langle n'\vec{k}|p_x|n\vec{k}\rangle [G(n\vec{k},n''\vec{k}';\epsilon-\omega-i\eta)\rho(n'''\vec{k}',n'\vec{k};\epsilon) + \rho(n\vec{k},n''\vec{k}';\epsilon) G(n'''\vec{k}',n'\vec{k};\epsilon+\omega+i\eta)] . \tag{2.10}$$

Upon taking the imaginary part of $S(\omega+i\eta)$, and making use of Eq. (2.9), one may demonstrate that the terms in $G_p\rho$ make no contribution to the imaginary part. After a bit of manipulation, we have

$$\mathrm{Im}[S(\omega+i\eta)] = \pi\,\mathrm{Re}\Big(\sum_{n,\ldots,n'''} \sum_{\vec{k}\vec{k}'} \int_{-\infty}^{+\infty} d\epsilon [f(\epsilon)-f(\epsilon+\omega)]\langle n''\vec{k}'|p_x|n'''\vec{k}'\rangle\langle n'\vec{k}|p_x|n\vec{k}\rangle \times \rho(n\vec{k},n''\vec{k}';\epsilon)\rho(n'''\vec{k}',n\vec{k};\epsilon+\omega)\Big) , \tag{2.11}$$

so for $\epsilon_2(\omega)$ we obtain a result that may be written

$$\epsilon_2(\omega) = \frac{4\pi^2 e^2}{Vm^2\omega^2}(1-e^{-\beta\omega}) \sum_{\vec{k}\vec{k}'} \sum_{n\ldots n'''} \int_{-\infty}^{+\infty} d\epsilon\, f(\epsilon)[1-f(\epsilon+\omega)]\,\mathrm{Re}[\langle n''\vec{k}'|p_x|n'''\vec{k}'\rangle\langle n'\vec{k}|p_x|n\vec{k}\rangle \times \rho(n\vec{k},n''\vec{k}';\epsilon)\rho(n'''\vec{k}',n'\vec{k};\epsilon+\omega)] \tag{2.12}$$

This is our general expression for $\epsilon_2(\omega)$. We proceed to apply the result to the model that will occupy us in Sec. III. This model is a two-band model, with a filled valence band that extends in energy from 0 to $-W_v$, and a conduction band that extends from E_g to E_g+W_c, where W_c and W_v are the width of the conduction band and valence band, respectively, with E_g the energy gap. The Hamiltonian $H=H_c+H_v$, that is we ignore mixing between host bands produced by the impurity. For this model, the spectral density $\rho(n\vec{k},n'\vec{k}';\epsilon)$ is diagonal in the band index. Then for both spectral densities to be nonzero, in the limit as the temperature $T\to 0$ we require ϵ to lie in the range $-W_v<\epsilon<0$ of the filled valence band, while the frequency ω is in the range $E_g<\omega<E_g+W_v+W_c$ where interband transitions are excited. We then have, with $\rho_v(\vec{k},\vec{k}';\epsilon)$ and $\rho_c(\vec{k}',\vec{k};\epsilon+\omega)$ the spectral densities in the conduction band and in the valence band (we let the

temperature $T \to 0$)

$$\epsilon_2(\omega) = \frac{4\pi^2 e^2}{Vm^2\omega^2} \sum_{\vec{k}\vec{k}'} \int_{-W_v}^{0} d\epsilon \, \mathrm{Re}[\langle v\vec{k}'|p_x|c\vec{k}'\rangle\langle c\vec{k}|p_x|v\vec{k}\rangle \rho_v(\vec{k},\vec{k}';\epsilon)\rho_c(\vec{k}',\vec{k};\epsilon+\omega)] . \tag{2.13}$$

Before we proceed, we pause to comment on one aspect of the work by Velicky and Levin,[2] and its relation to the present study. The point is of some generality, and not influenced by the differences in the models explored in their paper and in ours.

While the result in Eq. (2.13) will be applied to a material with a single impurity in the present paper, it can equally as well be applied to a substance with a finite concentration of impurities. In the latter case, one should average the product $\rho_v(\vec{k},\vec{k}';\epsilon)\rho_c(\vec{k}',\vec{k};\epsilon+\omega)$ over all possible impurity configurations. We denote this average by the angular brackets $\langle\cdots\rangle$. Velicky and Levin proceed by replacing the average of the product by the product of the average. That is, they write

$$\langle \rho_v(\vec{k},\vec{k}';\epsilon)\rho_c(\vec{k}',\vec{k};\epsilon+\omega)\rangle \cong \langle \rho_v(\vec{k},\vec{k}';\epsilon)\rangle\langle \rho_c(\vec{k}',\vec{k};\epsilon+\omega)\rangle . \tag{2.14a}$$

But one has $\langle \rho_v(\vec{k},\vec{k}';\epsilon)\rangle = \delta_{\vec{k}\vec{k}'}\bar{\rho}_v(\vec{k},\epsilon)$, and similarly for $\langle \rho_c(\vec{k}',\vec{k};\epsilon+\omega)\rangle$, so Eq. (2.13) becomes

$$\epsilon_2(\omega) = \frac{4\pi^2 e^2}{Vm^2\omega^2} \sum_{\vec{k}} |\langle v\vec{k}|p_x|c\vec{k}\rangle|^2 \times \int_{-W_v}^{0} d\epsilon \, \bar{\rho}_v(\vec{k},\epsilon)\bar{\rho}_c(\vec{k},\epsilon+\omega) . \tag{2.14b}$$

where $\bar{\rho}_v$ and $\bar{\rho}_c$ are real. The final step in Ref. 2 is to employ the coherent potential approximation to compute the averaged one-electron spectral densities $\bar{\rho}_v$ and $\bar{\rho}_c$.

The method in Ref. 2 replaces the alloy with spatial disorder by an average medium that is translationally invariant. The electron sees the impurities through an "optical potential" constructed through the CPA. In our view, such a treatment overlooks one feature of optical absorption in disordered solids that may be important, particularly in the dilute limit.

In Figs. 1(a) and 1(b), we illustrate schematically

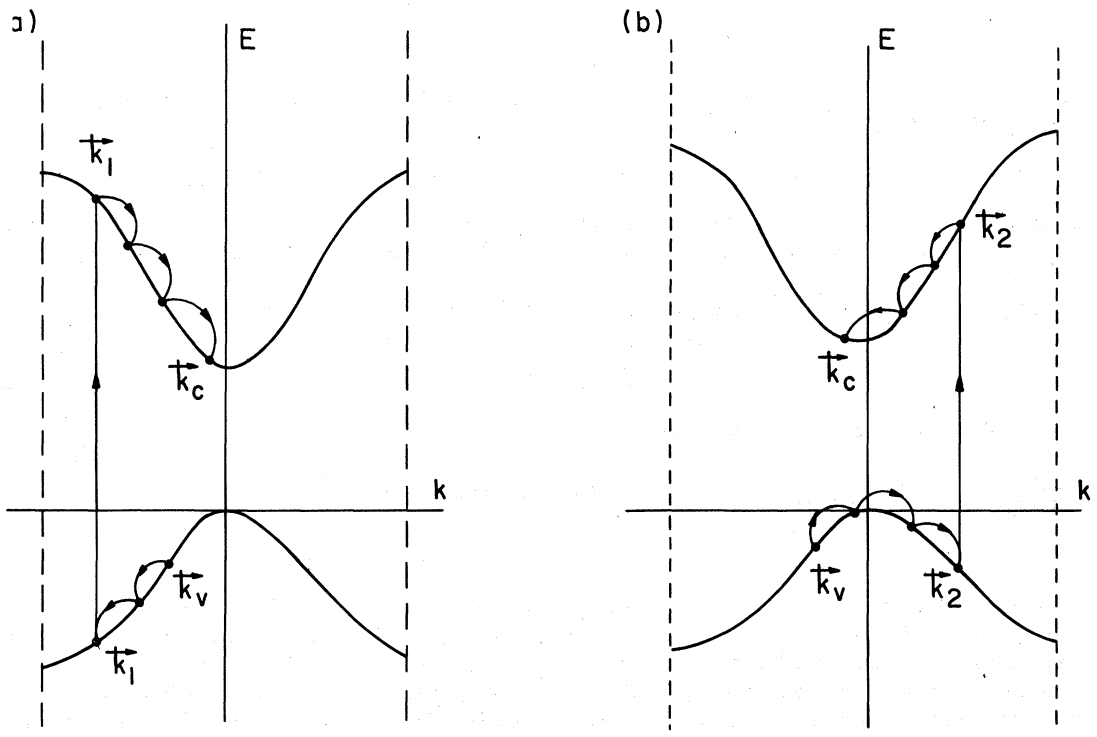

FIG. 1. Two distinct processes which contribute to optical absorption by indirect transitions in disordered solids. The intraband processes illustrated are produced by the impurity potential, and the interband transition is produced by the $\vec{p}\cdot\vec{A}$ term in the Hamiltonian. Since these two processes connect the same initial and final states, they interfere coherently in the absorption process.

two physically distinct processes which connect an initial state $\vec{k}_v$ in the valence band with $\vec{k}_c$ in the conduction band, where $\vec{k}_c \neq \vec{k}_v$. Since these two processes connect the same initial and final states, they necessarily interfere coherently. This is why Eq. (2.13) contains the product $\langle v\vec{k}'|p_x|c\vec{k}'\rangle\langle c\vec{k}|p_x|v\vec{k}\rangle$ with $\vec{k}' \neq \vec{k}$. One may appreciate from Eq. (2.14) that the decoupling scheme used by Velicky and Levin drops these interference effects from the theory. We believe these interference effects are surely present and influential in the dilute limit, where the various plane waves which are combined to produce the wave function of the electron near the impurity are coherent in phase, since they are mixed into the wave function by an impurity potential at a fixed position in the lattice. In more concentrated alloys (such as those examined by Velicky and Levin), these coherence effects may well be unimportant, since the presence of a finite impurity concentration leads to interference between waves scattered from different impurities. These interference effects may tend to "wipe out" the coherence effects.

The remarks above are framed in language appropriate to interband transitions in an insulator. For electrons in a metal, the decoupling scheme used by Velicky and Levin ignores the "scattering-in" terms that enter the Boltzmann equation. While these scattering-in terms do not contribute in the dilute limit for the model explored in Ref. 2, which has s-wave phase shifts only, in general their contribution is the same order of magnitude as the terms retained. We are presently recalculating the optical-absorption spectrum for the model used in Ref. 2, with the purpose of comparing the results of a one-impurity calculation with theirs, for the same model.

We return to the two-band model that forms the basis of the present paper. For the Hamiltonian of the electrons in the valence (conduction) band $H_{v(c)}$, we take the form

$$H_{v(c)} = \sum_{\vec{k}} \epsilon_{v(c)}(\vec{k}) C^{\dagger}_{\vec{k}} C_{\vec{k}} + \frac{V_{v(c)}}{N} \sum_{\vec{k}\vec{k}'} C^{\dagger}_{\vec{k}} C_{\vec{k}'} , \quad (2.15)$$

which describes a single impurity placed at the origin of the coordinate system. The valence electrons see an effective potential of strength V_v, and the conduction electrons see one of strength V_c.

The Green's functions for the conduction band and for the valence band will be denoted by $G_c(\vec{k},\vec{k}';z)$ and $G_v(\vec{k},\vec{k}';z)$, respectively. For the model, these have the well known Slater-Koster form

$$G_{v(c)}(\vec{k},\vec{k}';z) = \delta_{\vec{k}\vec{k}'} G^{(0)}_{v(c)}(\vec{k};z) + \Delta G_{v(c)}(\vec{k},\vec{k}';z) , \quad (2.16)$$

where

$$G^{(0)}_{v(c)}(\vec{k},z) = [\epsilon_{v(c)}(\vec{k}) - z]^{-1} , \quad (2.17a)$$

$$\Delta G^{(0)}_{v(c)}(\vec{k},\vec{k}';z) = -[V_{v(c)}/N] G^{(0)}_{v(c)}(\vec{k},z) G^{(0)}_{v(c)}(\vec{k}',z) \times [1 + V_{v(c)} F_{v(c)}(z)]^{-1} \quad (2.17b)$$

where

$$F_{v(c)}(z) = \frac{1}{N} \sum_{\vec{k}} \frac{1}{\epsilon_{v(c)}(\vec{k}) - z} \quad (2.17c)$$

The Green's functions in Eq. (2.16) and Eqs. (2.17) in combination with the expression for $\epsilon_2(\omega)$ in Eq. (2.13) will form the basis of the discussion of Sec. III.

III. APPLICATION OF THE THEORY TO A SIMPLE MODEL INSULATOR

To proceed further, we need not only the form of the one-electron Green's function [Eq. (2.16) and Eq. (2.17)], but we also need the form of the momentum matrix element $\langle v\vec{k}|p_x|c\vec{k}\rangle$. In this paper, we explore a simple two-band model of an insulating solid. The conduction band is presumed a simple tight-binding band with wave functions constructed from atomic s orbitals localized near each lattice site,

$$\langle \vec{x}|c\vec{k}\rangle = \frac{1}{\sqrt{N}} \sum_{\vec{l}} \varphi_s(\vec{x} - \vec{l}) e^{i\vec{k}\cdot\vec{l}} \quad (3.1)$$

while the valence band is constructed from atomic p_x orbitals:

$$\langle \vec{x}|v\vec{k}\rangle = \frac{1}{\sqrt{N}} \sum_{\vec{l}} \varphi_{p_x}(\vec{x} - \vec{l}) e^{i\vec{k}\cdot\vec{l}} . \quad (3.2)$$

If we ignore overlap between atomic orbitals centered on different sites, then a short calculation shows

$$\langle c\vec{k}|p_x|v\vec{k}\rangle = \langle s|p_x|p_x\rangle \quad (3.3)$$

independent of $\vec{k}$, where

$$\langle s|p_x|p_x\rangle = \int d^3x\, \varphi_s(\vec{x}) p_x \varphi_{p_x}(\vec{x}) . \quad (3.4)$$

Then we have

$$\epsilon_2(\omega) = \frac{4\pi^2 e^2}{V m^2 \omega^2} |\langle s|p_x|p_x\rangle|^2 \times \sum_{\vec{k}\vec{k}'} \int_{-W_v}^{0} d\epsilon\, \rho_v(\vec{k},\vec{k}';\epsilon) \rho_c(\vec{k}',\vec{k};\epsilon+\omega) . \quad (3.5)$$

From the form of the Green's function $G_{v(c)}(\vec{k},\vec{k}';\epsilon)$ given at the end of Sec. II, one finds the spectral density function may be written

$$\rho_{v(c)}(\vec{k},\vec{k}';\epsilon) = \delta_{\vec{k}\vec{k}'} \delta(\epsilon_{v(c)}(\vec{k}) - \epsilon) + (1/N) \Delta\rho_{v(c)}(\vec{k},\vec{k}';\epsilon) , \quad (3.6)$$

where

$$\Delta\rho_{v(c)}(\vec{k},\vec{k}';\epsilon)=\frac{V_{v(c)}}{2\pi i}\left(\frac{1}{1+V_{v(c)}F_{v(c)}(\epsilon-i\eta)}\,\frac{1}{\epsilon_{v(c)}(\vec{k})-\epsilon+i\eta}\,\frac{1}{\epsilon_{v(c)}(\vec{k}')-\epsilon+i\eta}\right.$$
$$\left.-\frac{1}{1+V_{v(c)}F_{v(c)}(\epsilon+i\eta)}\,\frac{1}{[\epsilon_{v(c)}(\vec{k})-\epsilon-i\eta][\epsilon_{v(c)}(\vec{k}')-\epsilon-i\eta]}\right). \tag{3.7}$$

When Eq. (3.6) is inserted into Eq. (3.5), we obtain four distinct terms. The first describes the interband absorption in the host, and the second three describe the impurity-induced (wave-vector-nonconserving) portions. We write the expression for $\epsilon_2(\omega)$ in the form

$$\epsilon_2(\omega)=\epsilon_2^{(0)}(\omega)+(1/N)[\epsilon_2^{(Ic)}(\omega)+\epsilon_2^{(Iv)}(\omega)+\epsilon_2^{(Icv)}], \tag{3.8}$$

where

$$\epsilon_2^{(0)}(\omega)=(4\pi^2e^2/Vm^2\omega^2)\,|\langle s|p_x|p_x\rangle|^2$$
$$\times\sum_{\vec{k}}\delta(\epsilon_v(\vec{k})-\epsilon_c(\vec{k})+\omega) \tag{3.9}$$

is the contribution of the pure matrix to $\epsilon_2(\omega)$, and the three terms $\epsilon_2^{(Ic)}(\omega)$, $\epsilon_2^{(Iv)}(\omega)$, and $\epsilon_2^{(Icv)}(\omega)$ when summed give the absorption induced by a single impurity. We have (for $E_g<\omega<E_g+W_v+W_c$)

$$\epsilon_2^{(Ic)}(\omega)=(4\pi^2e^2/Vm^2\omega^2)\,|\langle s|p_x|p_x\rangle|^2$$
$$\times\sum_{\vec{k}}\Delta\rho_c(\vec{k},\vec{k};\epsilon_v(\vec{k})+\omega), \tag{3.8a}$$

$$\epsilon_2^{(Iv)}(\omega)=(4\pi^2e^2/Vm^2\omega^2)\,|\langle s|p_x|p_x\rangle|^2$$
$$\times\sum_{\vec{k}}\Delta\rho_v(\vec{k},\vec{k};\epsilon_c(\vec{k})-\omega), \tag{3.8b}$$

and

$$\epsilon_2^{(Icv)}(\omega)=(4\pi^2e^2/Vm^2\omega^2)\,|\langle s|p_x|p_x\rangle|^2(1/N)$$
$$\times\sum_{\vec{k},\vec{k}'}\int d\epsilon\,\Delta\rho_v(\vec{k},\vec{k}';\epsilon)\Delta\rho_c(\vec{k}'\vec{k};\epsilon+\omega). \tag{3.8c}$$

In Sec. II of the present paper, we noted that the decoupling scheme of Velicky and Levin ignores certain interference effects in the theory. These interference effects are contained only in the term $\epsilon_2^{(Icv)}(\omega)$.

The terms which describe impurity-induced absorption do not appear to simplify into forms that enable their structure to be analyzed in a general way. As a result, to proceed, one requires a specific model of each of the two bands. In this paper, we consider the simplest possible model that can be explored in some detail: a one-dimensional material for which

$$\epsilon_v(\vec{k})=-\tfrac{1}{2}W_v(1-\cos ka_0) \tag{3.9a}$$

and

$$\epsilon_c(\vec{k})=E_g+\tfrac{1}{2}W_c(1-\cos ka_0), \tag{3.9b}$$

where W_v is the width of the valence band, W_c that of the conduction band, a_0 the lattice constant, and E_g the energy gap.

This model has the virtue that many of the functions which enter the theory may be evaluated in closed analytic form. In one dimension, at the band edges, the one-electron density of states exhibit square-root singularities. We may expect indirect impurity-induced transitions between these critical points [say between the bottom of the valence band ($k=\pi/a_0$) and the bottom of the conduction band ($k=0$)] to produce particulary sharp structure in $\epsilon_2(\omega)$.

The model may be of practical interest, since real three-dimensional crystals have sharp peaks in their density of states, in a manner that mimics the one-dimensional solid.[8] Indeed, these materials may be useful ones to study optically, to examine effects similar to those discussed here.

For the model, it is a simple matter to obtain a closed-form expression for $\epsilon_2^{(0)}(\omega)$. One finds, if we imagine our model material to be a collection of linear structures with n_s lines per unit area,

$$\epsilon_2^{(0)}(\omega)=(4\pi n_se^2/m^2\omega^2a_0)$$
$$\times\frac{|\langle s|p_x|p_x\rangle|^2}{(\omega-E_g)^{1/2}(E_g+W_c+W_v-\omega)^{1/2}}. \tag{3.10}$$

The interband absorption feature shows the characteristic one-dimensional square-root singularity at the absorption edge $\omega=E_g$, and at the upper cutoff $\omega=E_g+W_c+W_v$ as well.

We pause to cast Eq. (3.10) in dimensionless form. The same convention will be used in the remainder of the paper. Let

$$\omega=xE_g, \tag{3.11a}$$

$$W_c=f_cE_g, \tag{3.11b}$$

$$W_v=f_vE_g. \tag{3.11c}$$

Furthermore, Eq. (3.10) can be written, after use of Eqs. (3.11),

$$\epsilon_2^{(0)}=\bar{\epsilon}r_0(x)x^{-2}, \tag{3.12}$$

where

$$\bar{\epsilon} = (4\pi n_s e^2/m^2 a_0 E_g^3)\,|\langle s|p_x|p_x\rangle|^2 \tag{3.13}$$

and

$$r_0(x) = [1/(x-1)^{1/2}(1+f_c+f_v-x)^{1/2}]\,. \tag{3.14}$$

Save for the singularities at $x=1$ and $x=1+f_e+f_v$, $r_0(x)$ is smooth and featureless through the region of allowed interband absorption.

To compute the impurity-induced absorption, we require the function $F_{v(c)}(\epsilon \pm i\eta)$, where $F_{v(c)}(\epsilon)$ is defined in Eq. (2.17c). A short integration shows

$$F_v(\epsilon \pm i\eta) = \begin{cases} [\epsilon(\epsilon+W_v)]^{-1/2}, & \epsilon < -W_v \\ \pm i[-\epsilon(\epsilon+W_v)]^{-1/2}, & -W_v < \epsilon < 0 \\ -[\epsilon(\epsilon+W_v)]^{-1/2}, & \epsilon > 0\,, \end{cases} \tag{3.15}$$

with a similar expression for $F_c(\epsilon \pm i\eta)$.

Through use of Eq. (3.15), and the analogous expression for $F_c(\epsilon \pm i\eta)$, both $\epsilon_2^{(Ic)}(\omega)$ and $\epsilon_2^{(Iv)}(\omega)$ may be written in terms of an integral over energy of a function known analytically, for the model. For example, for $\epsilon_2^{(Iv)}(\omega)$, we can write

$$\epsilon_2^{(Iv)}(\omega) = \frac{\bar{\epsilon} a_0 E_g^3 V_v}{4\pi i \omega^2} \int_{-\pi/a_0}^{+\pi/a_0} dk \left(\frac{1}{1+V_v F_v(\epsilon_c(k)-\omega-i\eta)} \frac{1}{[\epsilon_v(k)-\epsilon_c(k)+\omega+i\eta]^2} \right.$$
$$\left. - \frac{1}{1+V_v F_v(\epsilon_c(k)-\omega+i\eta)} \frac{1}{[\epsilon_v(k)-\epsilon_c(k)+\omega-i\eta]^2} \right). \tag{3.16}$$

This may be expressed in terms of an integral over $\epsilon = \epsilon_c(k)$ by noting the relation, valid for our simple model,

$$\epsilon_v(k) = (W_v/W_c)[E_g - \epsilon_c(k)]\,. \tag{3.17}$$

We write $\epsilon_2^{(Iv)}(\omega)$ in the form

$$\epsilon_2^{(Iv)}(\omega) = \bar{\epsilon} r^{(Iv)}(x) x^{-2}\,, \tag{3.18}$$

with a similar definition of $r^{(Ic)}(x)$, and also $r^{(Icv)}(x)$.

We turn first to a description of our numerical studies of $r^{(Iv)}(x)$, $r^{(Ic)}(x)$, and $r^{(Icv)}(x)$. Before we present these results, we comment on the procedure used to evaluate the integrals which follow from Eq. (3.16). The integrals are quite tricky to evaluate, because of the singular terms $[\epsilon_v(k) - \epsilon_c(k) + \omega + i\eta]^{-2}$ which give difficulty for photon frequencies in the range $E_g < \omega < E_g + W_c + W_v$, where interband absorption is allowed.

Our basic strategy has been to evaluate Eq. (3.16) directly (after converting the integral to one on energy), with the parameter η kept small and finite. Values of η in the range of $10^{-3}W_v$ or $10^{-4}W_v$ were chosen for this purpose. A very fine mesh was employed, with care taken in the near vicinity of the singularity. We then tested all results by varying the value of η, to insure their insensitivity to the choice of η.

The integrals we encounter have the general structure

$$g(\epsilon_0) = \int_{\epsilon_m}^{\epsilon_M} \frac{d\epsilon\, f(\epsilon)}{(\epsilon - \epsilon_0 \pm i\eta)^2} \tag{3.19}$$

which we rearrange to read

$$g(\epsilon_0) = f(\epsilon_0) \int_{\epsilon_m}^{\epsilon_M} \frac{d\epsilon}{(\epsilon-\epsilon_0 \pm i\eta)^2} + \int_{\epsilon_m}^{\epsilon_M} \frac{[f(\epsilon)-f(\epsilon_0)]}{(\epsilon-\epsilon_0 \pm i\eta)^2}\, d\epsilon \tag{3.20a}$$

or integrating the first term explicitly,

$$g(\epsilon_0) = f(\epsilon_0)\left(\frac{1}{\epsilon_m - \epsilon_0} - \frac{1}{\epsilon_M - \epsilon_0}\right) + \int_{\epsilon_m}^{\epsilon_M} \frac{[f(\epsilon)-f(\epsilon_0)]}{[\epsilon-\epsilon_0 \pm i\eta]^2}\, d\epsilon\,. \tag{3.20b}$$

With the use of Eq. (3.20b), we could obtain reliable results for the numerical integrations, as $\eta \to 0$. The procedure works quite well, except when ϵ_0 is close to the upper or lower limit ϵ_M or ϵ_m of the integration, a situation of little interest to us.

In Fig. 2 we show the diagrams which contribute to the three terms $r^{(Iv)}$, $r^{(Ic)}$, and $r^{(Icv)}$. In $r^{(Iv)}$, the hole in the valence band scatters repeatedly from the impurity ($r^{(Iv)}$ begins with the term first order in V_v), while the final-state electron in the conduction band is unaffected by the impurity. Thus, $r^{(Iv)}$ depends on only V_v, and not V_c. The term $r^{(Ic)}$ describes contributions where the conduction electron scatters repeatedly off the impurity, with the hole unaffected. As a consequence $r^{(Ic)}$ depends only on V_c, with its first contribution proportional to V_c. Finally, $r^{(Icv)}$ sums all processes in which both the electron and the hole scatter from the impurity. The lowest-order contributions to $r^{(Icv)}$ are proportional to the product $V_c V_v$, so both scattering potentials must act for $r^{(Icv)}$ to be nonvanishing.

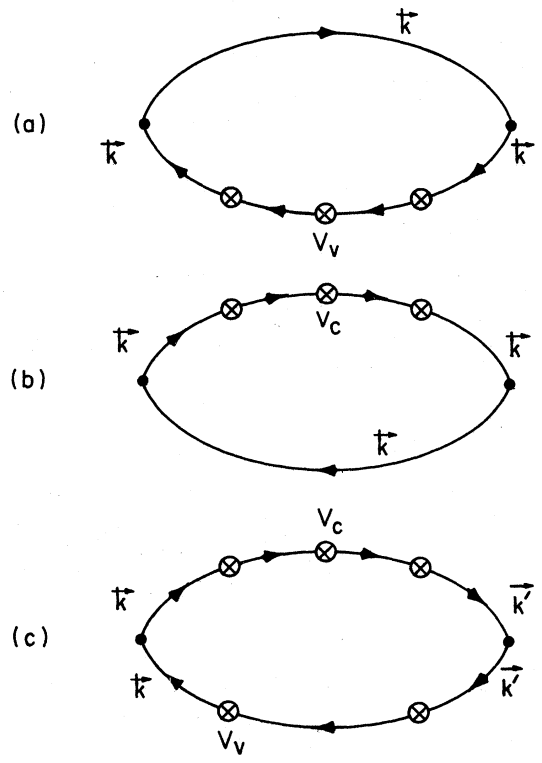

FIG. 2. (a) Diagrams which contribute to $r^{(Iv)}$. (b) The diagrams which contribute to $r^{(Ic)}$. (c) The diagrams which contribute to $r^{(Icv)}$; there must be at least one scattering event in both the electron and the hole line, for a diagram to contribute to $r^{(Icv)}$.

In all the calculations reported below, we have chosen $W_v = E_g$ and $W_c = 2W_v$. In terms of the reduced photon frequency x defined in Eq. (3.11a), the region of allowed interband absorption extends from $x=1$ to $x=4$. Dimensionless measures of the impurity potentials are the ratios V_v/W_v and V_c/W_v.

In Fig. 3(a), we present the results of our calculation of $r^{(Iv)}(x)$, for the case where a repulsive potential $V_v = +2W_v$ acts on the hole in the valence band. One sees a background absorption rather similar to that from the host matrix [Eq. (3.12)]. Superimposed on this background are two well-defined features, one very near $x=2$ and one near $x=3$. These features are structure that arises from impurity-induced indirect transitions between critical points in the host band structure, as we shall see. For the calculations in Fig. 3(a), we have set $\eta = 2\times10^{-3}W_v$, as indicated in the figure. In Fig. 3(b), we show a high-resolution study of the structure near $x=2$, with $\eta = 10^{-4}W_v$. Comparison of this curve with a similar one for $\eta = 2\times10^{-4}W_v$ shows we have reached the point where the principal features of the structure are insensitive to η. We believe that in the limit $\eta \to 0$, this structure is a step discontinuity in the absorption constant; as η is decreased, the structure approaches a step discontinuity.

In Fig. 4, we illustrate the indirect transitions responsible for the structure in Fig. 3. The feature near $x=2$ arises from transitions between the bottom of the valence band (at the zone boundary) and the bottom of the conduction band (near the zone center). The feature near $x=3$ has its origin in impurity-induced transitions between the top of the valence band (zone center) and the top of the conduction band (zone boundary).

We remark that the *sign* of $r^{(Iv)}(x)$ is controlled by that of the potential V_v. If we change the sign of V_v, the sign of $r^{(Iv)}(x)$ is changed also. From this remark, and the remaining results presented below, it is evident that impurity-induced struc-

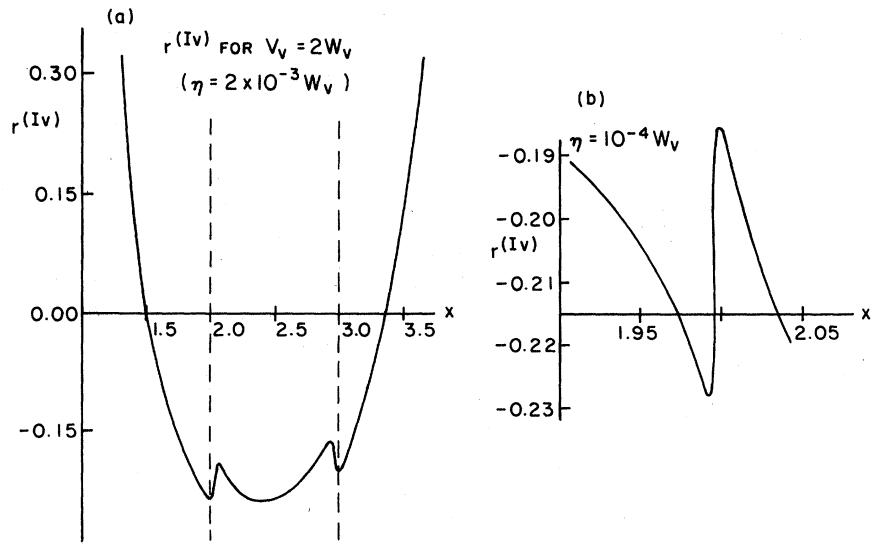

FIG. 3. (a) Function $r^{(Iv)}(x)$, for the case where $V_v = 2W_v$, and $W_v = E_g$, $W_c = 2W_v$. As indicated, the value of η was fixed at $\eta = 2\times10^{-3}$. (b) The detail in $r^{(Iv)}(x)$ near $x=2$, for $\eta = 10^{-4}\ W_v$.

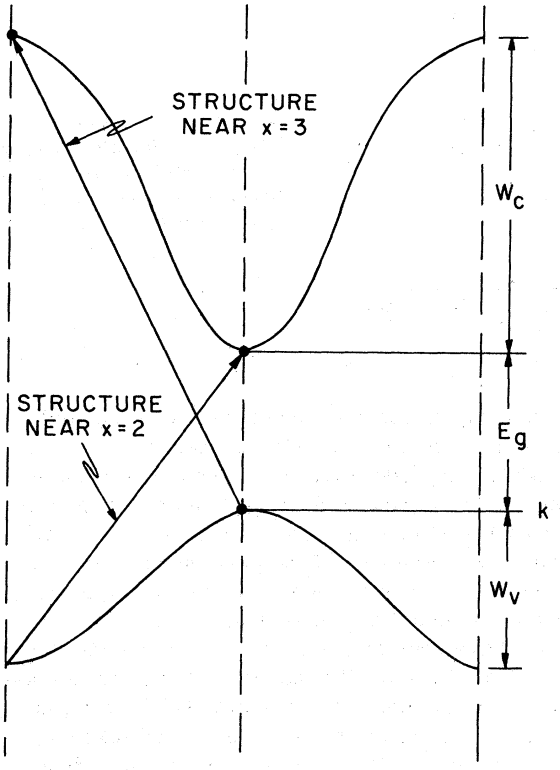

FIG. 4. Illustration of the indirect transitions responsible for the structures present in Fig. 3.

ture in $\epsilon_2(\omega)$ marks the energy difference between pairs of critical points in the host band structure, but the shape of the feature depends on the details of the impurity potential.

In Fig. 5(a), we show a plot of the function $r^{(Ic)}(x)$, for the case where the potential in the conduction band is repulsive (as in the valence band), with the value $V_c = +\frac{1}{2}W_c$. The general shape of $r^{(Ic)}(x)$ is quite similar to that of $r^{(Iv)}(x)$, save for a difference in overall sign. We shall appreciate the reason for this from an argument presented in Sec. IV. On the scale of Fig. 5(a), we see no structure at $x=2$ and $x=3$, as in Fig. 3(a). As one sees from Fig. 5(b), a high-resolution scan of the region near $x=2$ shows structure present similar to that in Fig. 3(a), with inverted sign. The size of the feature is quite sensitive to the strength of the potential, but we always find a feature small compared to that displayed in Fig. 3. The reason why the structure is much less prominent here is that the potential seen by the electron in the conduction band has been taken very much weaker than that seen by the valence electron. As remarked above, a dimensionless measure of the strength of the potentials is provided by the ratios V_c/W_v and V_c/W_c. The calculations in Figs. 3 and 5 have been performed for $V_v/W_v = 2$, and $V_c/W_c = \frac{1}{2}$, respectively.

Finally, in Figs. 6(a) and 6(b), we show the behavior of the term $r^{(Icv)}(x)$, for which both V_c and V_v must be nonzero. The calculations are carried out for $V_v = 2W_v$ and $V_c = \frac{1}{2}W_c$. In Fig. 7(b), a high-resolution calculation shows a clear shoulder is present in $r^{(Icv)}(x)$ at $x=2$; the shape of the feature here is quite distinctly different than either that in $r^{(Iv)}(x)$ or that in $r^{(Ic)}(x)$.

In Fig. 7(a), we plot the function $r_0(x)$ that controls the absorption in the host matrix, while in Fig. 7(b), for the case $V_v = 2W_v$ and $V_c = \frac{1}{2}W_c$, we combine the earlier results to display the total impurity-induced contribution to the absorption constant. The features at $x=2$ and $x=3$, which for these parameters receive their dominant contribution from $r^{(Iv)}$, are clearly visible.

IV. GENERAL REMARKS

From the results of Sec. III, we see that placing an impurity in a solid can "activate" critical points in the optical density of states not accessible by studies of the pure matrix. We believe the syste-

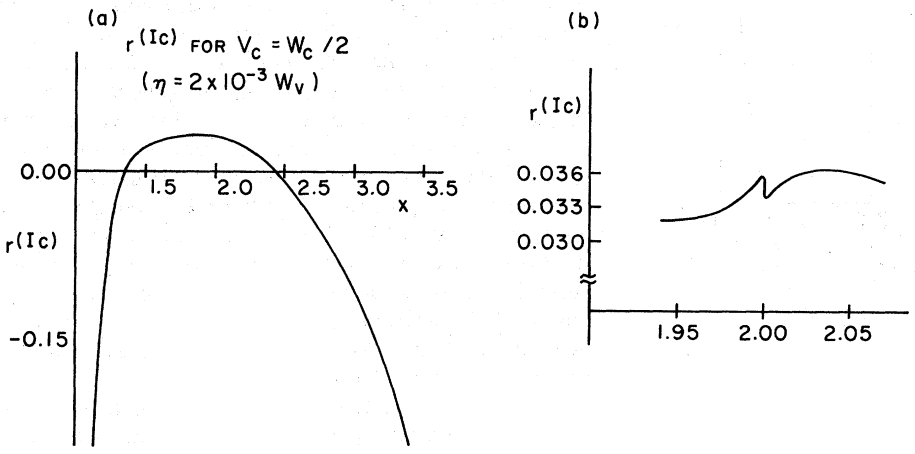

FIG. 5. (a) Calculation of $r^{(Ic)}(x)$ for the case $V_c = \frac{1}{2}W_c$ and (b) a high-resolution study of $r^{(Ic)}(x)$ near $x=2$.

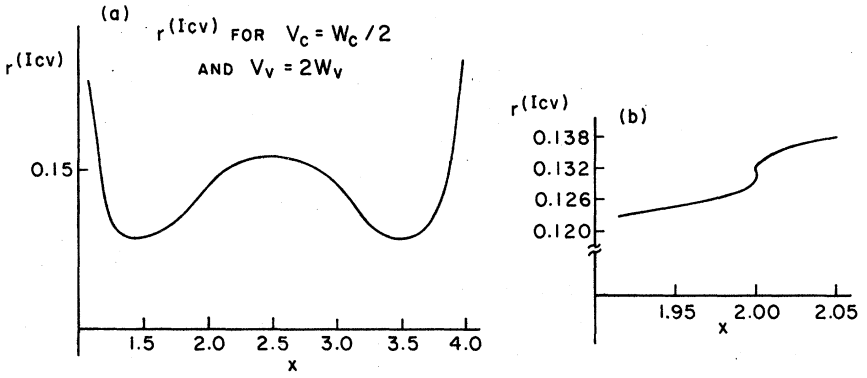

FIG. 6. (a) Function $r^{(Icv)}(x)$ as a function of x, for $V_c = \frac{1}{2}W_c$ and $V_v = 2W_v$. (b) A high-resolution numerical study of $r^{(Icv)}(x)$ near $x = 2$.

matic experimental study of such features may prove a most useful supplement to the conventional optical studies of nominally pure solids. The features we find for our simple model are clear and distinctive, but they are also of modest magnitude, even for the rather strong impurity potentials used in the calculations. The various methods of derivative spectroscopy may prove a useful means of probing such structures.

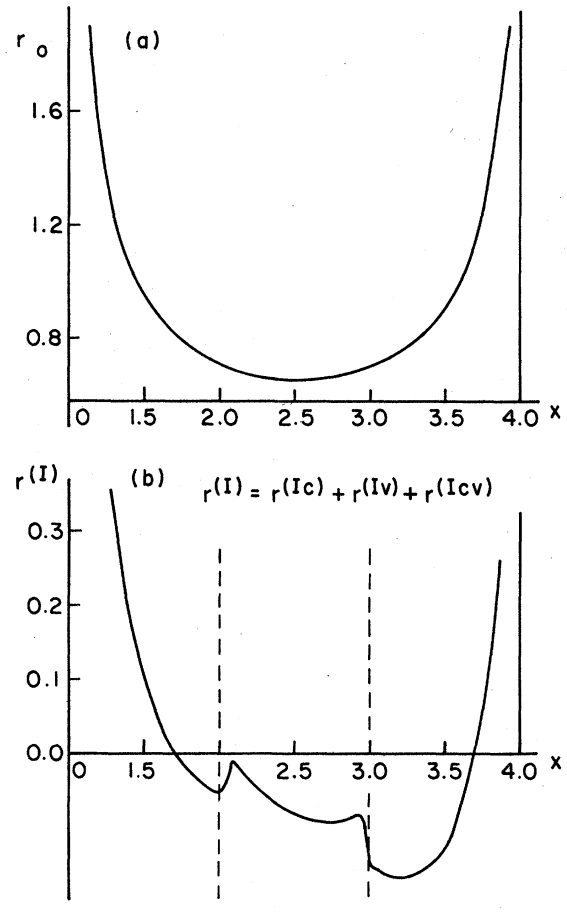

FIG. 7. (a) Function $r_0(x)$, which describes the optical absorption in the pure matrix (b) the sum of $r^{(Ic)}(x)$, $r^{(Iv)}(x)$, and $r^{(Ivc)}(x)$ for the case $V_v = 2W_v$ and $V_c = \frac{1}{2}W_c$.

While the model that forms the basis of the numerical calculations displayed in Sec. III is a very special one, nonetheless from its study we can infer some features of the phenomenon we expect to be more general. We conclude the paper with brief comments on some of these points.

We have seen that both the magnitude and the shape of the impurity-induced features in the optical spectrum depend on the details of the impurity potential, for our example. If we had taken V_c large enough, with a decrease in V_v, then from Figs. 3, 5, and 6 it is quite evident that the structures near $x = 2$ and $x = 3$ would have a shape very different than that apparent in Fig. 7. Little in general can be said about the *shape* of such features from knowledge of the host band structure alone, although the *position* of the structures clearly is controlled by the host band structure.

The most naive phenomenology would suppose that the impurity-induced indirect transitions would give a contribution to $\epsilon_2(\omega)$ which is proportional to the joint density of states $\rho_T(\omega)$ defined by

$$\rho_T(\omega) = \int d\epsilon \rho_v(\epsilon)\rho_c(\epsilon + \omega)\,, \tag{4.1}$$

where the integral is over the initial states allowed to participate in the absorption process by energy conservation alone. The comments in the preceding paragraph show clearly that in general, we do not expect this to be the case, since we find the *shape* of the structure clearly depends on the details of the impurity potentials. To illustrate this explicitly, we plot in Fig. 8 the joint density of states for our model near $x = 2$. The shape of the feature in the joint density of states bears no resemblence to the structure in any of the three impurity-induced structures in $\epsilon_2(\omega)$, so in no case we have explored do we find structures similar to the joint density of states.

We can also see that the structure induced by the impurity does not appear in the spectrum when the

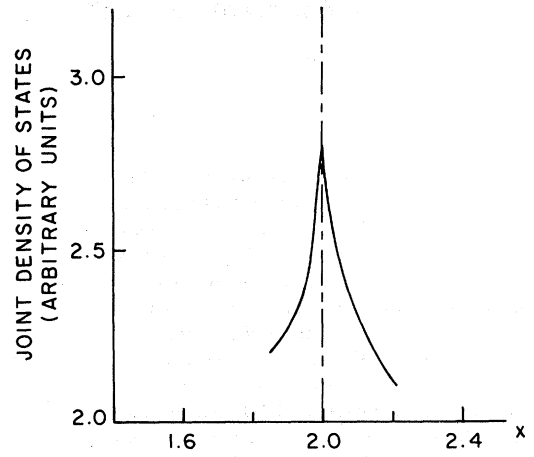

FIG. 8. Joint density of states for the model near $x = 2$.

impurity potential is sufficiently weak that its effect can be described by the lowest order of perturbation theory. To see this, consider the impurity contribution to $\epsilon_2(\omega)$ first order in V_v and V_c. This contribution comes from $r^{(Ic)}$ and $r^{(Iv)}$, and upon isolating the lowest-order contribution to each, we find for the impurity-induced contribution to $\epsilon_2(\omega)$ the result

$$\epsilon_2^{(I)}(\omega) = \frac{1}{N}(V_v - V_c)\frac{\partial}{\partial\omega}\epsilon_2^{(0)}(\omega)\,. \tag{4.2}$$

The result in Eq. (4.2) is precisely that expected from the rigid-band theory of alloys; the effect of the impurity is to shift the energy of each valence-band level by the amount V_v/N, and each conduction-band level by V_c/N. To see "activation" of critical points by the impurity, the impurity potentials must be strong enough for the rigid-band theory to break down. We believe this emphasizes the importance of dilute alloy calculations such as that presented here, where the calculation treats the influence of the impurity potential exactly, at the expense of examining the effect of finite concentrations.

We note that the result in Eq. (4.2), while valid only in perturbation theory, shows a repulsive potential acting on the final-state electron has an opposite effect of one which acts on the initial state. This is consistent with the calculations displayed in Figs. 3 and 5.

ACKNOWLEDGMENTS

We are both grateful to Professor H. D. Drew for a number of stimulating discussions of this problem. One of the authors (J.C.P.) is grateful to the NSF for financial support.

---

*Supported by Grant No. AFOSR 76-2887 of the Air Force Office of Scientific Research, Office of Aerospace Research, U.S.A. F.

†Permanent address: Laboratoire de Structure Electronique des Solides (ERA-CNRS No. 100), Université Louis Pasteur, Strasbourg, France.

[1]For a theoretical discussion of infrared absorption by lattice vibrations in impure crystals, see A. A. Maradudin, in *Astrophysics and The Many Body Problem* (Benjamin, New York, 1963), p. 253. Experimental Raman data which illustrate the point in question here have been presented by S. Ushioda [Solid State Commun. 15, 149 (1974)].

[2]B. Velicky and K. Levin, Phys. Rev. B 2, 938 (1970).

[3]B. Caroli, Phys. Kondens. Mater. 1, 346 (1963).

[4]For studies of the CuNi system, and other alloys where a virtual level plays a key role, see, H. D. Drew and R. E. Doezema, Phys. Rev. Lett. 28, 1581 (1972); B. Y. Lao, R. E. Doezma, and H. D. Drew, Solid State Commun. 15, 1253 (1974); and D. Beaglehole, Phys. Rev. B 14, 341 (1976).

[5]B. Kjöllerström, Philos. Mag. 19, 1207 (1969).

[6]A. J. Bennett and D. Penn, Phys. Rev. B 11, 3644 (1975).

[7]M. Tokumoto, H. D. Drew, and A. Bagchi (unpublished).

[8]For example of a model explicitly based on this notion, see, J. Labbé and J. Friedel, J. Phys. Radium 27, 153 (1966); 27, 303 (1966); 27, 708 (1966).